Title
Lack of Cas13a inhibition by anti-CRISPR proteins from Leptotrichia prophages

Journal
Molecular Cell, 82(11)

ISSN
1097-2765

Authors
Johnson, Matthew C
Hille, Logan T
Kleinstiver, Benjamin P
et al.

Publication Date
2022-06-01

DOI
10.1016/j.molcel.2022.05.002

Peer reviewed

HHS Public Access

Author manuscript

Mol Cell. Author manuscript; available in PMC 2023 June 02.

Published in final edited form as:

Mol Cell. 2022 June 02; 82(11): 2161–2166.e3. doi:10.1016/j.molcel.2022.05.002.

Lack of Cas13a inhibition by anti-CRISPR proteins from *Leptotrichia* prophages

Matthew C. Johnson[1], **Logan T. Hille**[2,3,4], **Benjamin P. Kleinstiver**[3,4,5], **Alexander J Meeske**[6,+], **Joseph Bondy-Denomy**[1,7,8,9,+]

[1]Department of Microbiology and Immunology, University of California, San Francisco, San Francisco, CA 94158, USA

[2]PhD Program in Biological and Biomedical Sciences, Harvard University, Boston, MA, 02115, USA

[3]Center for Genomic Medicine, Massachusetts General Hospital, Boston, MA, 02114, USA

[4]Department of Pathology, Massachusetts General Hospital, Boston, MA, 02114, USA

[5]Department of Pathology, Harvard Medical School, Boston, MA, 02115, USA

[6]Department of Microbiology, University of Washington, Seattle, WA 98109, USA

[7]Quantitative Biosciences Institute, University of California, San Francisco, San Francisco, CA 94158, USA

[8]Innovative Genomics Institute, Berkeley, CA 94720, USA

[9]Lead contact

Summary

CRISPR systems are prokaryotic adaptive immune systems that use RNA-guided Cas nucleases to recognize and destroy foreign genetic elements. To overcome CRISPR immunity, bacteriophages have evolved diverse families of anti-CRISPR proteins (Acrs). Recently, Lin et al. (2020) described the discovery and characterization of 7 Acr families (AcrVIA1–7) that inhibit type VI-A CRISPR systems. We detail several inconsistencies that question the results reported in the Lin et al. (2020) study. These include inaccurate bioinformatics analyses, and bacterial strains that are impossible to construct. Published strains were provided by the authors, but MS2 bacteriophage plaque assays did not support the published results. We also independently tested

[+] Co-corresponding authors: Meeske@uw.edu, Joseph.Bondy-Denomy@ucsf.edu.

Author contrubutions. Conceptulization, J.B.P.; Formal analysis M.C.J., L.T.H., B.P.K. and A.J.M.; Writing – Review & Editing, M.C.J., L.T.H., B.P.K., A.J.M and J.B.P.

Declaration of interests. J.B.-D. is a scientific advisory board member of SNIPR Biome and Excision Biotherapeutics and a scientific advisory board member and co-founder of Acrigen Biosciences. J.B.-D. is an inventor on patents filed by UCSF pertaining to anti-CRISPR technology. B.P.K is an inventor on patents and patent applications filed by Mass General Brigham that describe genome engineering technologies. B.P.K. consults for Avectas Inc., EcoR1 capital, and ElevateBio, and is an advisor to Acrigen Biosciences, Life Edit Therapeutics, and Prime Medicines.

the Acr sequences described in the original report, in *E. coli* and mammalian cells, but did not observe anti-Cas13a activity. Taken together, our data and analyses prompt us to question the claim that AcrVIA1–7 reported in Lin et al. are type VI anti-CRISPR proteins.

eTOC

Johnson et al. independently assayed the activity of 7 Type VI-A anti-CRISPRs (Acrs) published by Lin et al., (2020) but found no inhibition. The authors detail inconsistencies with the strains constructed by Lin et al. The authors do not believe these proteins are real Acrs.

Introduction

CRISPR-Cas systems provide their prokaryotic hosts with sequence-specific immunity against invading genetic elements, including bacteriophages and plasmids. To achieve immunity, short nucleotide sequences (spacers) are captured from foreign genomes and stored in the CRISPR locus, where they are transcribed and processed into small CRISPR RNAs (crRNAs) that guide the recognition and cleavage of elements matching the spacer. CRISPR systems are diverse and classified into six distinct types and 33 subtypes with different sequence content and mechanisms of interference (Makarova et al., 2020). Type VI CRISPR systems use the RNA-guided RNase Cas13 to recognize and cleave phage mRNA transcripts.

To overcome immunity, many phages encode small anti-CRISPR (Acr) proteins, which use different mechanisms to inhibit the binding and/or enzymatic activities of Cas proteins. Recently, Wu and colleagues (Lin et al. 2020) reported the discovery of seven type VI-A anti-CRISPRs (AcrVIA1-AcrVIA7) encoded by strains of *Leptotrichia* and *Rhodobacter* that inhibit Cas13a from *Leptotrichia wadei* (LwaCas13a), *Leptotrichia shahii* (LshCas13a), and *Leptotrichia buccalis* (LbuCas13a). The proteins were identified bioinformatically in prophages and tested with a series of assays including *in vitro* transcription-translation (Tx-Tl), phage and plasmid targeting assays. The authors demonstrated that these Acr proteins strongly inhibited Cas13a-mediated RNA knockdown and RNA editing in human cell lines. Separately, we (A.J.M) reported that an unrelated type VI Acr (called $\text{AcrVIA1}_{\text{Lse}}$) from a prophage of *Listeria seeligeri*, inhibits Cas13a from *Listeria seeligeri* (Meeske et al., 2020).

We discovered numerous concerning issues within the approach and results of the Lin et al. 2020 study. Here, we summarize our concerns: (i) there is no bioinformatic evidence supporting the conclusion that AcrVIA1–7 from Lin et al. are anti-CRISPR proteins, (ii) several strains reported as being used for experiments in the paper are not possible to construct due to plasmid incompatibility, (iii) none of the seven proteins tested had anti-CRISPR activity against LwaCas13a or LbuCas13a in our own bacterial assays, and (iv) the two most potent reported proteins, AcrVIA4 and AcrVIA5, did not substantially inhibit LwaCas13a-mediated RNA knockdown in human cells.

Results

Lin et al. used bioinformatic strategies to identify type VI Acr candidates. Specifically, they searched public sequence databases for bacterial genomes that have type VI CRISPR-Cas loci with spacers targeting another region in the same genome (often referred to as "self-targeting spacers"). A spacer and its target should not be able to stably coexist in the same cell, therefore the presence of self-targeting spacers suggests that the CRISPR system might be inhibited by an anti-CRISPR protein encoded by a prophage residing in the same genome (Rauch et al., 2017). This approach has been successfully used to identify anti-CRISPRs for DNA-targeting type II and type V CRISPR systems (Marino et al., 2018; Rauch et al., 2017; Watters et al., 2018), but not previously applied for Type VI systems, which require a transcribed target in the correct orientation for basepairing (Abudayyeh et al., 2016; Meeske et al., 2019). Lin et al. identified a single strain of *Leptotrichia wadei* (str. F0279) that possessed three self-targeting spacers associated with its type VI-A CRISPR system. Next, the authors identified three prophage regions in the *L. wadei* F0279 genome and looked for candidate anti-CRISPR genes within them. To narrow down the list of phage genes, the authors identified three genes encoding proteins with predicted helix-turn-helix (HTH) motifs, which they dub anti-CRISPR-associated (*aca*) genes (1 per prophage) and examined genes near the "*aca"* genes for anti-CRISPR activity. *aca* genes are so-named based on their genomic position being adjacent to known *acr* genes (Bondy-Denomy et al., 2013; Pawluk et al., 2014, 2016a, 2016b; Pinilla-Redondo et al., 2020). Mechanistically, Aca proteins repress *acr* expression (Birkholz et al., 2019; Osuna et al., 2020a; Stanley et al., 2019). In Fig. 1D of the original report, the authors incorrectly label these genes as "*aca1, aca2,* and *aca3*" which match the names of *aca* genes previously used for *acr* discovery. The newly identified genes in *L. wadei* prophages have no detectable similarity to *aca1-aca3* and thus, there is no bioinformatic basis to designate these genes *aca*s, and no basis to suggest the genes located nearby are *acr*s. Adjacent to these "*aca"* genes, the authors identified 5 putative type VI Acrs (*acrVIA1–5*) in the L. wadei F0279 genome. The ORF depictions in Fig. 1D also mask the true size of the genes and the spacing between them, which we have re-drawn to scale (Fig. 1).

Two additional type VI *acrs* (*acrVIA6, acrVIA7*) were identified by looking at genes adjacent to homologs of known *acr* genes harbored by bacterial strains also possessing type VI CRISPR loci. The discovery of *acrVIA6* was based on a nearby gene described as a homolog of the previously discovered *acrIC1* (Marino et al., 2018) (Fig. 2A). Using BLASTp with default parameters against the nr database does not present this protein, which has few identifiable homologs. Alignments were not provided in the original report to show the basis for the conclusion of homology. We were able to recreate that stated 34.8% identity between AcrIC1 and the proposed homolog using pairwise BLASTp that calculated 8/23 identical residues (34.78%) but to only 12% of the query protein (E-value = 0.002) (Fig. 2B) and therefore conclude that the gene schematized $acrIC1_{Rca}$ is misinterpreted as an *acrIC1* homolog. Similarly, the authors indicate that *acrIIA1* and *acrIIC4* homologs in *Leptotrichia buccalis* str. DSM1135 led them to *acrVIA7*. Using the AcrIIC4 sequence (Lee et al., 2018) for BLASTp against the nr database does not present homologs in this isolate. But again, we were able to recreate the erroneous identity value of 58.8% using pairwise BLASTp

(10/17 residues align, over 29% of the protein) (Fig. 2C). We could not identify an AcrIIA1 homolog (Rauch et al., 2017) in this strain.

We conclude that every *acr* gene candidate was identified under unusual presuppositions, either through the selection of random HTH-containing proteins in prophages (*acrVIA1–5*, Fig. 1D in the original paper) and labeling them as *aca* genes with incorrect names (i.e., *aca1, aca2, aca3*), or through the identification of incorrect homologs of known *acr* genes (*acrVIA6–7* and *acrIB1* in Fig. 4B in the original paper).

Despite the lack of bioinformatic evidence, it remained possible that the seven candidate proteins identified by Lin et al. were indeed Acr proteins, as demonstrated through multiple experimental approaches in the original report. To test them experimentally, we first sought to reproduce the findings from the original study using the authors' published reagents. All of the Acr proteins were shown by Lin et al. to inhibit Cas13a-mediated interference against the *E. coli* RNA bacteriophage MS2. To reproduce this experiment, bacterial strains possessing three different vectors expressing LwaCas13a or LbuCas13a, an MS2-targeting guide, and an Acr protein were procured from the authors, pre-constructed in the C3000 background. Of the 19 strains received, 14 grew on the prescribed antibiotics (Amp, Strep, Amp) and plaque assays were conducted. Our MS2 phage lysate formed robust plaques on an independently sourced *E. coli* C3000 host strain with no vectors present. On the provided strains with either Cas13a and a non-targeting guide expressed, faint phage-induced clearings were observed, which were absent when a targeting guide was provided, suggesting some functional immunity (Fig. 3). However, the targeting strain with the added empty "Acr vector" displayed robust plaquing on the LwaCas13 strain. Moreover, none of the strains harboring plasmids expressing the putative AcrVIA proteins restored MS2 plaque formation, suggesting either a lack of activity, or plasmid incompatibility (described below). On most strains, we observed faint clearings, but importantly this could not be attributed to anti-CRISPR activity as the respective control strains with empty Acr vectors had phage growth. Together, we did not observe Cas13a inhibition using the strains provided by Lin et al with this MS2 challenge assay.

We sought to reconstruct the strains ourselves with plasmids that were provided, but immediately realized that the strains cannot be constructed as described in the original study. MS2 phage infects the *E. coli* strain C3000, and each of the published strains contains three plasmids: (i) either an LwaCas13a or LbuCas13a expression plasmid in the vector backbone p2CT (these were generated by the Doudna lab and deposited in Addgene); (ii) an MS2-targeting guide RNA plasmid in vector backbone pCDFDuet; and (iii) an Acr expression plasmid in vector backbone pET16b. However, the p2CT backbone (East-Seletsky et al., 2016) and pET16b backbone are incompatible plasmids containing the same antibiotic resistance marker (Amp) and the same origin of replication. Therefore, these strains are challenging to construct. Second, both of these backbones are designed for T7 RNA polymerase-driven gene expression for protein purification and are normally used in DE3-lysogenized host strains containing a copy of T7 RNAP (Studier et al., 1990). Strain C3000, a K12 derivative, has no copy of T7 RNAP, and therefore cannot drive expression of Cas13a nor the Acr.

Another method that Lin et al used to demonstrate Acr activity was a plasmid transformation assay in *E. coli*. Cas13a restricts the transformation of plasmids expressing target RNA, while AcrVIA1–5 were shown to relieve this restriction. Again, we encountered difficulty when trying to repeat the experiments as performed in the original study. The experiment described by Lin et al involves the use of a "self-targeting" Cas13a (LwaCas13a, LbuCas13a, or LshCas13a) plasmid, which contains a guide RNA targeting a gentamicin resistance gene on the same plasmid. However, such a self-targeting Cas13 plasmid should not be possible to construct in the first place, unless *cas13a* or the gentamicin resistance gene were conditionally expressed. The paper contains no information about how any of the plasmids were constructed, and there is no description of an inducible promoter used in this plasmid. We requested the strain carrying this plasmid from the corresponding author, and although it was listed among the shipped strains, we were unable to culture it in the specified antibiotics.

To independently test whether the seven proteins alleged to be type VI Acr proteins inhibit Cas13a, we performed plasmid transformation assays in *E. coli*. We designed plasmids carrying either LbuCas13a or LwaCas13a crRNAs targeting the kanamycin resistance marker of a second plasmid (Fig. 4A). To test Cas13a function, we first transformed strains harboring each Cas13a plasmid (or empty vector) with the kanR plasmid. As expected, we found that both Cas13a homologs prevented transformation with the targeted plasmid in a crRNA-dependent manner (Fig. 4B, no Acr control). To test the putative Acrs, we synthesized *E. coli* codon-optimized alleles of each gene (*acrVIA1–7*) and cloned them into the target plasmid under the control of a Ptet promoter (Fig. 4A). In contrast to the robust Cas13a inhibition reported by Lin et al, we found that none of the seven proteins reduced Cas13a targeting (Fig. 4B). As a positive control to ensure Acrs can inhibit Cas13a in this assay, we generated an LseCas13a plasmid targeting the same antibiotic resistance marker in a plasmid harboring $AcrVIA1_{Lse}$ (Meeske et al. 2020). While LseCas13a was capable of strongly interfering with a target plasmid lacking the Acr, the $AcrVIA1_{Lse}$ target plasmid was completely resistant to LseCas13a. All of the Acrs in this experiment were expressed from the same vector backbone, using the same promoter and ribosome binding site. All of the Cas13a homologs and crRNA expression constructs were similarly matched. We therefore conclude that AcrVIA1–7 exhibit little or no anti-CRISPR activity against LbuCas13a or LwaCas13a in bacteria.

Lastly, we sought to recapitulate the author's demonstration of potent inhibition of LwaCas13a in human cells with the putative AcrVIA proteins. Lin et al. report near-complete inhibition of LwaCas13a transcript degradation by AcrVIA5 and high levels of inhibition for several other candidate AcrVIAs. We performed experiments in HEK 293T cells with LwaCas13a and the Lin et al. crRNAs targeting endogenous *KRAS* and *PPIB* transcripts (Figs. 5A and 5B, respectively), in the absence or presence of varying amounts of plasmids encoding their two most potent reported AcrVIA proteins, AcrVIA5 and AcrVIA4. As negative controls, we also examined AcrIIA4 and AcrIIA5 that inhibit Cas9 and are not expected to inhibit Cas13a enzymes (Fig. 5). Across the various quantities of Acr plasmids that we examined, RT-qPCR analysis at 48-hours post-transfection revealed largely inconsequential reduction of transcript degradation by AcrVIA5 or AcrVIA4; inhibition was not meaningfully different than what we observed in the presence of the negative control

AcrIIA4 or AcrIIA5 that should not interact with LwaCas13a. In our experiments, the highest doses of AcrVIA4 or AcrVIA5 expression plasmid were a 4.3x excess molar ratio relative to the LwaCas13a expression plasmid, which is comparable to the approximately 5.7x excess reported by Lin et al. For context, using similar construct architectures (plasmid backbones, promoters, codon usage, etc.) we previously demonstrated that AcrIIA4 and AcrIIA5 exhibit robust inhibition of SpCas9 at AcrIIA:Cas9 plasmid molar ratios as low as 0.1x (Mahendra et al., 2020; Osuna et al., 2020b). Together, our results do not support the conclusion from Lin et al. that AcrVIA5 and AcrVIA4 strongly inhibit LwaCas13a activity in human cells.

Here, we have presented multiple lines of evidence to challenge the findings put forth by Lin et al. (2020) pertaining to the discovery of seven Type VI-A Acr proteins. Bioinformatic inconsistencies are detailed, along with plasmid incompatibilities and independent experiments that could not establish the functionality of these proteins.

We acknowledge a limitation of this study being that we lack an inhibitor against these Cas13 enzymes as a positive control. We also acknowledge that we don't have access to all the original materials that were utilized in the Lin et al. 2020 paper

STAR METHODS

RESOURCE AVAILABILITY

Further information and requests for reagent and resource sharing should be directed to and will be fulfilled by the lead contact Dr. Joe Bondy-Denomy (Joseph.Bondy-Denomy@ucsf.edu). Plasmids generated in this have been deposited to Addgene 171128 and 171129. This study did not generate any original code or data.

EXPERIMENTAL MODEL AND SUBJECT DETAILS

Bacterial strains—Bacteria were grown in Lysogeny Broth (LB) with or without antibiotics and grown at 37°C.

Human cells—Human HEK 293T cells (ATCC) were cultured in Dulbecco's Modified Eagle Medium (DMEM) supplemented with 10% heat-inactivated FBS (HI-FBS) and 1% penicillin/streptomycin. Supernatants from cell cultures were tested monthly for mycoplasma using MycoAlert PLUS (Lonza).

METHOD DETAILS

Bacterial strains and plasmid preparation—Plasmid culture and extraction, as well as plasmid transformation assays were performed with New England Biolabs Turbo Competent E. coli. Bacteria were grown in Lysogeny Broth (LB) supplemented with antibiotics: kanamycin (50 μg/mL), chloramphenicol (25 μg/ml), and anhydrotetracyline (100 ng/mL). 0.2% arabinose was added to induce expression of Cas13 from Para promoters.

Human cells culture and transfections—For transfections, approximately 2×10^4 cells per well were seeded in 96-well plates. Approximately 18–22 hours after seeding,

transfections were performed using TransIT-X2 (Mirus) transfection reagent with 60 ng of LwaCas13a plasmid (Addgene ID 91924), 20 ng of gRNA plasmid (generated by cloning oligos into an LwaCas13a crRNA entry plasmid, LTH151, Addgene ID 171129), and with 0, 2, 12, or 72 ng of Acr plasmid. The human codon optimized Acr constructs for AcrVIA4 and AcrVIA5 were synthesized by Twist Biosciences and cloned into a pCMV backbone (plasmid IDs LTH956 and LTH957 respectively; see Supplementary Table 2), similar to how we previously generated the human cell expression constructs for AcrIIA4 and AcrIIA5 (Addgene IDs 133801 and 133802, respectively) (see Supplementary Table 2). The total amount of DNA in each transfection remained constant (152 ng), with a pCMV-null plasmid (Addgene ID 171128) used to balance DNA amounts when titrating the Acr plasmid. The plasmid mixtures were combined with 0.54 ul of TransIT-X2 and volume of Opti-MEM (ThermoFisher) to a final volume of 15 ul, incubated at room temperature for 15 minutes, and then applied to the HEK 293T cells. All experiments were performed with 3 independent biological replicates.

Plasmid construction—Cas13 plasmids for transformation assay were cloned into the vector pAM38 containing p15A origin of replication, chloramphenicol resistance marker, and an arabinose-inducible Para promoter. Coding sequences for LwaCas13a, LbuCas13a, or LseCas13a were inserted downstream of the Para promoter, and crRNA constructs were inserted downstream of the cas13 coding sequence driven by a synthetic promoter (J23119). These plasmids were constructed by three piece Gibson assembly as described below and validated by Sanger sequencing. Lists of plasmids, oligonucleotide primers, and crRNAs can be found in Supplementary Tables.

LwaCas13a plasmids: Three piece Gibson assembly using (1) SalI/HindIII-digested pAM38, (2) LwaCas13a coding sequence and Shine-Dalgarno sequence amplified from Addgene #91865 using primers oAM1496 and oAM1497, and (3) J23119-driven crRNA gBlock fragments synthesized by IDT was used to generate pAM491 (LwaCas13a kan crRNA) and pAM494 (LwaCas13a non-targeting crRNA).

LbuCas13a plasmids: Three piece Gibson assembly using (1) SalI/HindIII-digested pAM38, (2) LbuCas13a coding sequence codon-optimized for E. coli (synthesized by Genewiz) and Shine-Dalgarno sequence amplified using primers oAM211 and oAM1477, and (3) J23119-driven crRNA gBlock fragments synthesized by IDT was used to generate pAM492 (LbuCas13a kan crRNA) and pAM475 (LbuCas13a non-targeting crRNA).

LseCas13a plasmids: Three piece Gibson assembly using (1) SalI/HindIII-digested pAM38, (2) LseCas13a coding sequence codon-optimized for E. coli (synthesized by Genewiz) and Shine-Dalgarno sequence amplified using primers oAM207 and oAM994, and (3) J23119-driven crRNA gBlock fragments synthesized by IDT was used to generate pAM526 (LseCas13a kan crRNA) and pAM319 (LseCas13a non-targeting crRNA).

Acr plasmids: Acrs were expressed from pAM326 (carrying kanamycin resistance marker and pWV01 origin of replication) and driven by an anhydrotetracycline-inducible Ptet promoter. Acr coding sequences were synthesized by Genewiz, amplified using primers oAM1529 and oAM1530, and inserted with Ptet fragment into HindIII/EagI-digested

pAM326 via three piece Gibson assembly to make pAM495 (AcrVIA1), pAM496 (AcrVIA2), pAM497 (AcrVIA3), pAM498 (AcrVIA4), pAM499 (AcrVIA5), pAM500 (AcrVIA6), pAM501 (AcrVIA7). The AcrVIA1Lse plasmid pAM383 was generated previously (Meeske et al. 2020).

Plasmid transformation assay—NEB Turbo competent E. coli were transformed with either empty vector or plasmids harboring LwaCas13a, LbuCas13a, or LseCas13a and expressing non-targeting or targeting crRNAs, and selected on LB agar containing chloramphenicol and 0.2% glucose to repress Cas13a expression. Each transformed strain was made chemically competent by resuspension of exponentially growing cells in $\frac{1}{5}$ culture volume of ice cold TFB I (10 mM CaCl2,30 mM potassium acetate, pH 5.8, 100 mM RbCl, 50mM MnCl2, 15% glycerol), incubation on ice for 15 minutes, then pelleting and resuspension in 1/25 culture volume of ice cold TFB II (10 mM MOPS pH 6.5, 10 mM RbCl, 75 mM CaCl2, 15% glycerol). Chemically competent cells were transformed by heat shock at 42°C with 100 ng Acr plasmids or empty vector control, then recovered for 1 hour in LB. Tenfold serial dilutions of recovered transformants were made and 5 μL of each dilution was spotted onto LB agar supplemented with kanamycin, chloramphenicol, arabinose, and anhydrotetracycline. Plates were photographed after 1 day of incubation at 37°C.

RNA extraction and RT-qPCR—At 48 hours post-transfection, total RNA was extracted from transfected cells using an RNeasy Plus Mini Kit (Qiagen; cat. no. 74136). Purified RNA was reverse transcribed using a High-Capacity RNA-to-cDNA kit (ThermoFisher; cat. no. 4388950) using up to 250 ng of RNA as input. Prior to qPCR, the cDNA library for each sample was diluted 1:20. Samples for qPCR were prepared in technical triplicate with 5 ul of Fast SYBR Green Master Mix (ThermoFisher; cat. no. 4385610), 3 ul diluted cDNA, and 2 ul qPCR primer pairs specific to the target (IDT; Supplementary Table 1). Control reactions amplifying ACTB were set up in parallel for each cDNA library. Reaction cycling was performed using a Roche LightCycler480. To determine the fold change of each sample, the expression levels were normalized to a negative control transfection containing LwaCas13a plasmid and an empty pUC19 backbone plasmid (Addgene ID 133961). Each qPCR reaction was analyzed for purity by melting curve analysis to confirm a single PCR product.

MS2 phage assay—Strains were obtained from Lin et al, and grown in Lysogeny Broth (LB) supplied with ampicillin (100 μg/mL) and streptomycin (100 μg/mL) overnight at 37 °C. Cultures were diluted in 0.7% top agar and poured onto LB agar plates with 10 μM $MgSO_4$, 10 μM $CaCl_2$, ampicillin (100 μg/mL) and streptomycin (100 μg/mL). MS2 phage was plated in 10-fold dilution and incubated overnight at 30°C.

QUANTIFICATION AND STATISTICAL ANALYSIS

NCBI BLASTp tool was used with default parameters to determine protein homology between Lin et al. 2020 proteins and published anti-CRISPRs. RT-qPCR values were normalized to *ACTB* levels and performed in technical triplicates (n=3). Significance thresholds were set at p=0.05.

Supplementary Material

Refer to Web version on PubMed Central for supplementary material.

Acknowledgements

This work in the Bondy-Denomy lab (J.B.-D). is supported by the UCSF Program for Breakthrough Biomedical Research funded in part by the Sandler Foundation, the NIH [DP5-OD021344, R01GM127489], and DARPA HR0011-17-2-0043. M.J. is supported by the NSF GRFP Fellowship. B.P.K. acknowledges support from the Margaret Q. Landenberger Research Foundation and a Mass General Hospital Howard M. Goodman Fellowship. Work in the Meeske lab (A.J.M) is supported by the NIH [R35GM142460].

REFERENCES

Abudayyeh OO, Gootenberg JS, Konermann S, Joung J, Slaymaker IM, Cox DBT, Shmakov S, Makarova KS, Semenova E, Minakhin L, et al. (2016). C2c2 is a single-component programmable RNA-guided RNA-targeting CRISPR effector. Science 353, aaf5573. [PubMed: 27256883]

Abudayyeh O, Gootenberg J, Essletzbichler P et al. (2017). RNA targeting with CRISPR–Cas13. Nature 550, 280–284. [PubMed: 28976959]

Birkholz N, Fagerlund RD, Smith LM, Jackson SA, and Fineran PC (2019). The autoregulator Aca2 mediates anti-CRISPR repression. Nucleic Acids Res. 47, 9658–9665. [PubMed: 31428783]

Bondy-Denomy J, Pawluk A, Maxwell KL, and Davidson AR (2013). Bacteriophage genes that inactivate the CRISPR/Cas bacterial immune system. Nature 493, 429–432. [PubMed: 23242138]

East-Seletsky A, O'Connell MR, Knight SC, Burstein D, Cate JHD, Tjian R, and Doudna JA (2016). Two distinct RNase activities of CRISPR-C2c2 enable guide-RNA processing and RNA detection. Nature 538, 270–273. [PubMed: 27669025]

Lee J, Mir A, Edraki A, Garcia B, Amrani N, Lou HE, Gainetdinov I, Pawluk A, Ibraheim R, Gao XD, et al. (2018). Potent Cas9 Inhibition in Bacterial and Human Cells by AcrIIC4 and AcrIIC5 Anti-CRISPR Proteins. MBio 9.

Lin P, Qin S, Pu Q, Wang Z, Wu Q, Gao P, Schettler J, Guo K, Li R, Li G, et al. (2020). CRISPR-Cas13 Inhibitors Block RNA Editing in Bacteria and Mammalian Cells. Mol. Cell 78, 850–861.e5. [PubMed: 32348779]

Mahendra C, Christie KA, Osuna BA, Pinilla-Redondo R, Kleinstiver BP, and Bondy-Denomy J (2020). Broad-spectrum anti-CRISPR proteins facilitate horizontal gene transfer. Nat Microbiol 5, 620–629. [PubMed: 32218510]

Makarova KS, Wolf YI, Iranzo J, Shmakov SA, Alkhnbashi OS, Brouns SJJ, Charpentier E, Cheng D, Haft DH, Horvath P, et al. (2020). Evolutionary classification of CRISPR-Cas systems: a burst of class 2 and derived variants. Nat. Rev. Microbiol 18, 67–83. [PubMed: 31857715]

Marino ND, Zhang JY, Borges AL, Sousa AA, Leon LM, Rauch BJ, Walton RT, Berry JD, Joung JK, Kleinstiver BP, et al. (2018). Discovery of widespread type I and type V CRISPR-Cas inhibitors. Science 362, 240–242. [PubMed: 30190308]

Meeske AJ, Nakandakari-Higa S, and Marraffini LA (2019). Cas13-induced cellular dormancy prevents the rise of CRISPR-resistant bacteriophage. Nature 570, 241–245. [PubMed: 31142834]

Meeske AJ, Jia N, Cassel AK, Kozlova A, Liao J, Wiedmann M, Patel DJ, and Marraffini LA (2020). A phage-encoded anti-CRISPR enables complete evasion of type VI-A CRISPR-Cas immunity. Science.

Osuna BA, Karambelkar S, Mahendra C, Sarbach A, Johnson MC, Kilcher S, and Bondy-Denomy J (2020a). Critical Anti-CRISPR Locus Repression by a Bi-functional Cas9 Inhibitor. Cell Host Microbe 28, 23–30.e5. [PubMed: 32325051]

Osuna BA, Karambelkar S, Mahendra C, Christie KA, Garcia B, Davidson AR, Kleinstiver BP, Kilcher S, and Bondy-Denomy J (2020b). Listeria Phages Induce Cas9 Degradation to Protect Lysogenic Genomes. Cell Host Microbe 28, 31–40.e9. [PubMed: 32325050]

Pawluk A, Bondy-Denomy J, Cheung VHW, Maxwell KL, and Davidson AR (2014). A new group of phage anti-CRISPR genes inhibits the type I-E CRISPR-Cas system of Pseudomonas aeruginosa. MBio 5, e00896. [PubMed: 24736222]

Pawluk A, Staals RHJ, Taylor C, Watson BNJ, Saha S, Fineran PC, Maxwell KL, and Davidson AR (2016a). Inactivation of CRISPR-Cas systems by anti-CRISPR proteins in diverse bacterial species. Nature Microbiology 1, 1–6.

Pawluk A, Amrani N, Zhang Y, Garcia B, Hidalgo-Reyes Y, Lee J, Edraki A, Shah M, Sontheimer EJ, Maxwell KL, et al. (2016b). Naturally Occurring Off-Switches for CRISPR-Cas9. Cell 167, 1829–1838.e9. [PubMed: 27984730]

Pinilla-Redondo R, Shehreen S, Marino ND, Fagerlund RD, Brown CM, Sørensen SJ, Fineran PC, and Bondy-Denomy J (2020). Discovery of multiple anti-CRISPRs highlights anti-defense gene clustering in mobile genetic elements. Nat. Commun 11, 5652. [PubMed: 33159058]

Rauch BJ, Silvis MR, Hultquist JF, Waters CS, McGregor MJ, Krogan NJ, and Bondy-Denomy J (2017). Inhibition of CRISPR-Cas9 with Bacteriophage Proteins. Cell 168, 150–158.e10. [PubMed: 28041849]

Stanley SY, Borges AL, Chen K-H, Swaney DL, Krogan NJ, Bondy-Denomy J, and Studier FW, Rosenberg AH, Dunn JJ, Dubendorff JW (1990). Use of T7 RNA polymerase to direct expression of cloned genes. Methods Enzymol. 185:60–89 [PubMed: 2199796]

Davidson AR (2019). Anti-CRISPR-Associated Proteins Are Crucial Repressors of Anti-CRISPR Transcription. Cell 178, 1452–1464.e13. [PubMed: 31474367]

Watters KE, Fellmann C, Bai HB, Ren SM, and Doudna JA (2018). Systematic discovery of natural CRISPR-Cas12a inhibitors. Science 362, 236–239. [PubMed: 30190307]

Highlights

- Type VI-A Acrs published by Lin et al., possess no inhibition activity against Cas13a.
- Our independent assays could not validate these proteins as inhibitory in human cells.
- Poorly interpreted BLAST results may have led to the identification of these proteins.

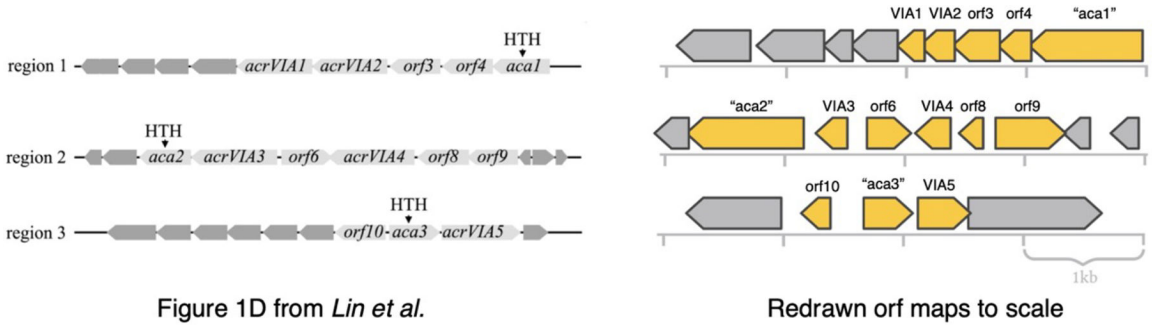

Figure 1:

Gene organization of reported Acrs. Misnamed *aca* genes and adjacent *acr* genes as depicted in Lin et al. 2020 (left) and with ORFs redrawn to reflect their true scale and spacing (right).

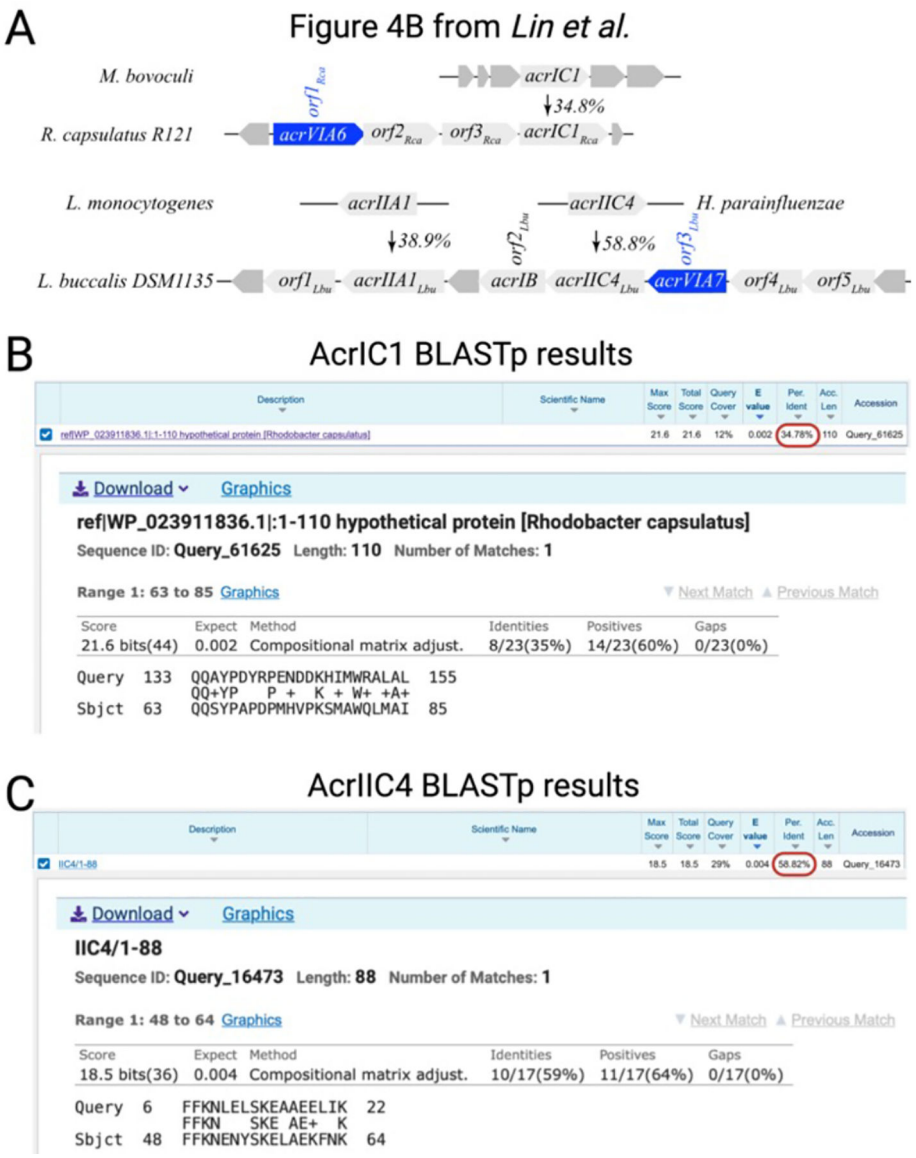

Figure 2:

Misidentification of Acr homologs. (**A**) Reported Acr homologs with percent identity for each match indicated in Lin et al. 2020. BLASTp alignments demonstrating no significant homologs are present in the target genomes for (**B**) AcrIC1 or (**C**) AcrIIC4.

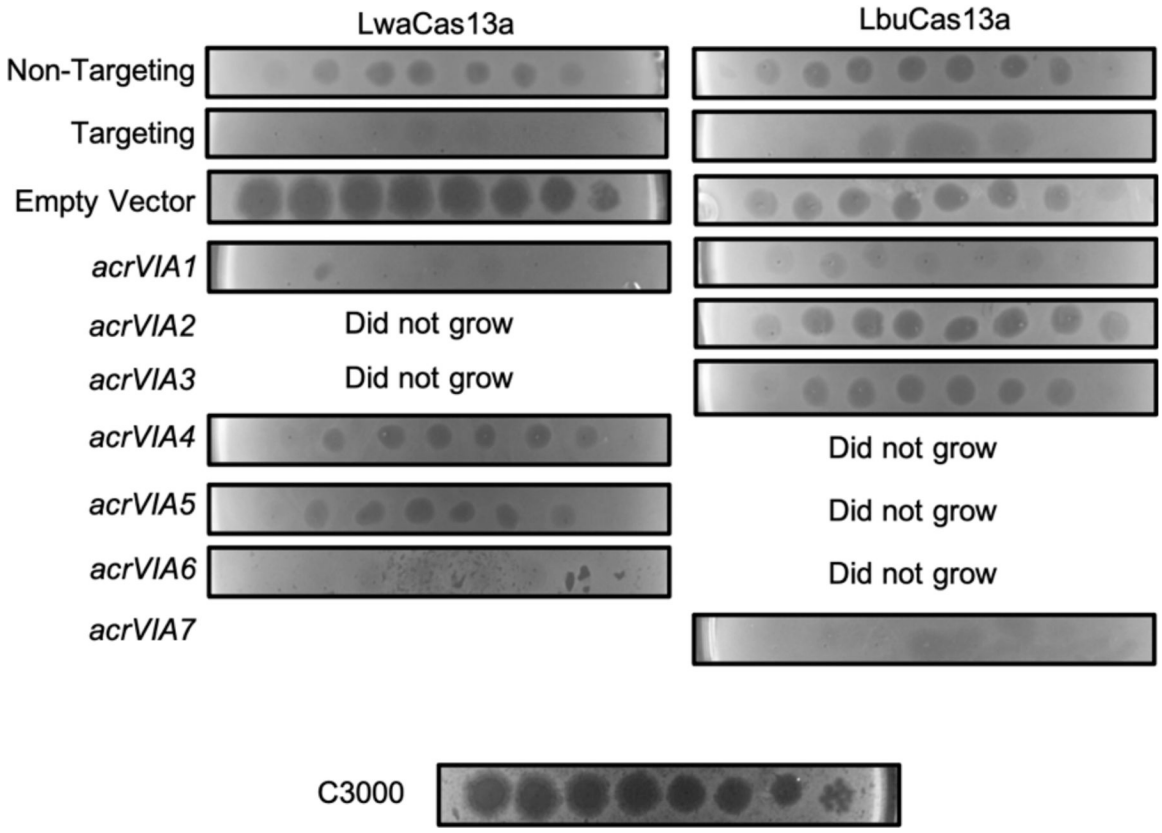

Figure 3:

Plaque assays with MS2 phage (10-fold dilutions from left to right) on lawns expressing LwaCas13a or LbuCas13a and a cognate crRNA targeting MS2. With the exception of the "non-targeting" strain, the others possess an MS2 targeting crRNA and either an empty pET16b plasmid, or one encoding *acrVIA1–7*, as indicated. Due to the inconsistent appearance of the clearings, an independently sourced C3000 wild-type strain was also procured, and plaque assays conducted to confirm the titer and robustness of the phage lysate.

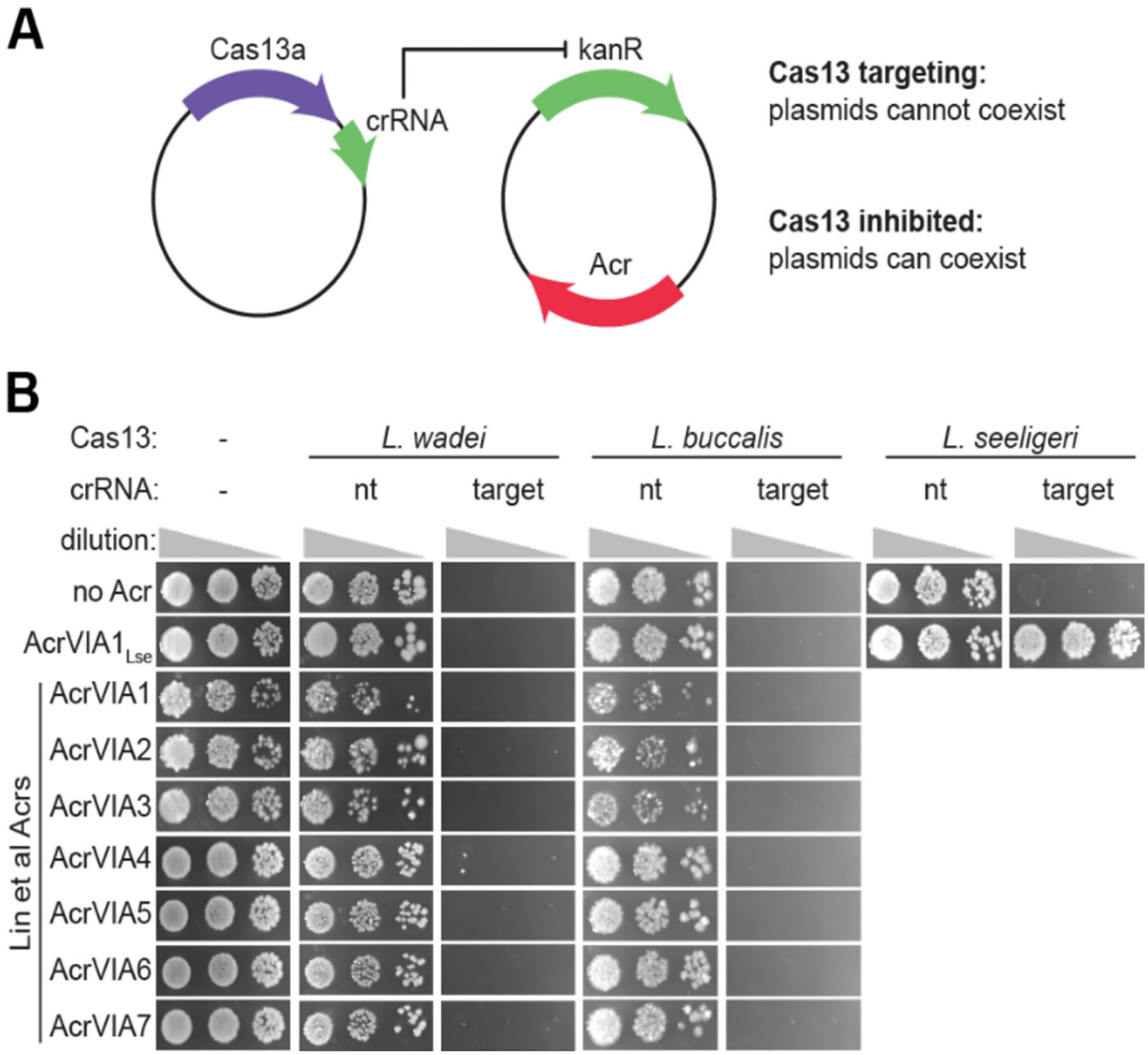

Figure 4: Target plasmid transformation assay to measure Acr function.

(**A**) Assay schematic. *E. coli* strains carried plasmids with Cas13a from *L. wadei*, *L. buccalis*, or *L. seeligeri* and a crRNA targeting the kanamycin resistance marker of a second plasmid (or non-targeting crRNA control), which also candidate Acr proteins. Cas13a targeting of the kanR marker restricts transformation of the target plasmid, unless the Acr inhibits Cas13a. (**B**) Results of transformation assay. The indicated recipient strains (columns) were transformed with the indicated plasmids (rows), serially diluted and spotted onto media selecting for both plasmids. nt, non-targeting crRNA.

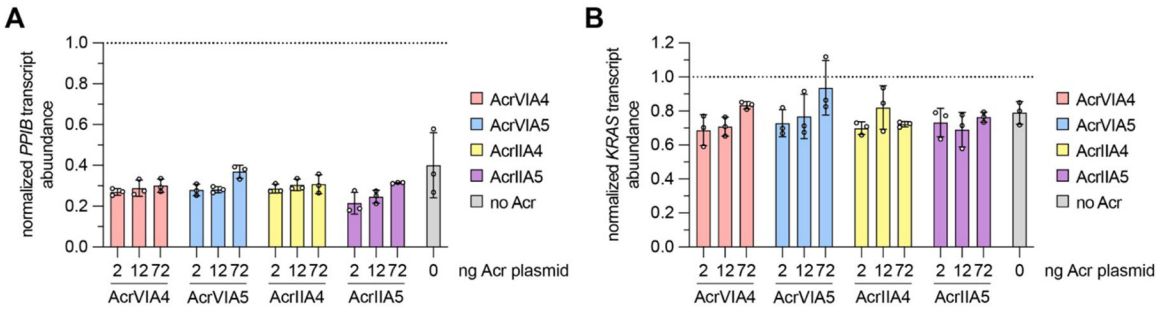

Figure 5: Assessment of AcrVIA-mediated inhibition of LwaCas13a.

(**A**, **B**) Knockdown of endogenous *PPIB* (**panel A**) or *KRAS* (**panel B**) transcripts by LwaCas13a in the presence of various amounts of Acr expression plasmids was determined via RT-qPCR analysis (n = 3 biological replicates; dots represent the mean of three technical triplicate qPCR values with SD shown). *PPIB* or *KRAS* RNA levels were normalized to *ACTB* and knockdown was determined by comparison to a non-targeting LwaCas13a control. Increasing amounts of plasmids encoding the anti-CRISPR proteins AcrVIA5, AcrVIA4, AcrIIA4, and AcrIIA5 were added to a consistent amount of LwaCas13a nuclease and gRNA plasmids. The molar ratios of the Acr to LwaCas13a expression plasmids were approximately 0.12, 0.72, and 4.32 for the 2 ng, 12 ng, and 72 ng treatments, respectively.

KEY RESOURCES TABLE

REAGENT or RESOURCE	SOURCE	IDENTIFIER
Bacterial and virus strains		
E. coli c-3000/p2CT-LwaCas13a/pCDFDuet-MS2 pre-crRNA/pET16b	Lin et al., 2020	LwaCas13a empty vector
E. coli c-3000/p2CT-LwaCas13a/pCDFDuet-MS2 pre-crRNA/pET16b-AcrVIA1	Lin et al., 2020	LwaCas13a AcrVIA1
E. coli c-3000/p2CT-LwaCas13a/pCDFDuet-MS2 pre-crRNA/pET16b-AcrVIA2	Lin et al., 2020	LwaCas13a AcrVIA2
E. coli c-3000/p2CT-LwaCas13a/pCDFDuet-MS2 pre-crRNA/pET16b-AcrVIA3	Lin et al., 2020	LwaCas13a AcrVIA3
E. coli c-3000/p2CT-LwaCas13a/pCDFDuet-MS2 pre-crRNA/pET16b-AcrVIA4	Lin et al., 2020	LwaCas13a AcrVIA4
E. coli c-3000/p2CT-LwaCas13a/pCDFDuet-MS2 pre-crRNA/pET16b-AcrVIA5	Lin et al., 2020	LwaCas13a AcrVIA5
E. coli c-3000/p2CT-LwaCas13a/pCDFDuet-MS2 pre-crRNA/pET16b-AcrVIA6	Lin et al., 2020	LwaCas13a AcrVIA6
E. coli c-3000/p2CT-LbuCas13a/pCDFDuet-LbuCas13a MS2 pre-crRNA/pET16b	Lin et al., 2020	LbuCas13a empty vector
E. coli c-3000/p2CT-LbuCas13a/pCDFDuet-LbuCas13a MS2 pre-crRNA/pET16b-AcrVIA1	Lin et al., 2020	LbuCas13a AcrVIA1
E. coli c-3000/p2CT-LbuCas13a/pCDFDuet-LbuCas13a MS2 pre-crRNA/pET16b-AcrVIA2	Lin et al., 2020	LbuCas13a AcrVIA2
E. coli c-3000/p2CT-LbuCas13a/pCDFDuet-LbuCas13a MS2 pre-crRNA/pET16b-AcrVIA3	Lin et al., 2020	LbuCas13a AcrVIA3
E. coli c-3000/p2CT-LbuCas13a/pCDFDuet-LbuCas13a MS2 pre-crRNA/pET16b-AcrVIA4	Lin et al., 2020	LbuCas13a AcrVIA4
E. coli c-3000/p2CT-LbuCas13a/pCDFDuet-LbuCas13a MS2 pre-crRNA/pET16b-AcrVIA5	Lin et al., 2020	LbuCas13a AcrVIA5
E. coli c-3000/p2CT-LbuCas13a/pCDFDuet-MS2 pre-crRNA/pET16b-AcrVIA7	Lin et al., 2020	LbuCas13a AcrVIA7
E. coli c-3000/p2CT-LwaCas13a/pCDFDuet-GenR pre-crRNA/pET16b	Lin et al., 2020	LwaCas13a targeting
E. coli c-3000/p2CT-LwaCas13a/pCDFDuet-GenR non-target pre-crRNA/pET16b	Lin et al., 2020	LwaCas13a non targeting
E. coli c-3000/p2CT-LbuCas13a/pCDFDuet-GenR pre-crRNA/pET16b	Lin et al., 2020	LbuCas13a targeting
E. coli c-3000/p2CT-LbuCas13a/pCDFDuet-GenR non-target pre-crRNA/pET16b	Lin et al., 2020	LbuCas13a non targeting
MS2 phage	Alexander J Meeske	MS2
E. coli C-3000	Alexander J Meeske	C3000
Experimental models: Cell lines		
Human HEK 293T cells	ATCC	HEK 293T
Recombinant DNA		
pAM491 CmR LwaCas13a kan crRNA	This paper	pAM491
pAM494 CmR LwaCas13a non-targeting crRNA	This paper	pAM494
pAM492 CmR LbuCas13a kan crRNA	This paper	pAM492
pAM475 CmR LbuCas13a non-targeting crRNA	This paper	pAM475
pAM526 CmR LseCas13a kan crRNA	This paper	pAM526

REAGENT or RESOURCE	SOURCE	IDENTIFIER
pAM319 CmR LseCas13a non-targeting crRNA	This paper	pAM319
pAM326 KanR and pWV01 origin of replication	This paper	pAM326
pAM495 (pAM326-AcrVIA1)	This paper	pAM495
pAM496 (pAM326-AcrVIA2)	This paper	pAM496
pAM497 (pAM326-AcrVIA3)	This paper	pAM497
pAM498 (pAM326-AcrVIA4)	This paper	pAM498
pAM499 (pAM326-AcrVIA5)	This paper	pAM499
pAM500 (pAM326-AcrVIA6)	This paper	pAM500
pAM501 (pAM326-AcrVIA7)	This paper	pAM501
pAM383 (pAM326-LseAcrVIA1)	Meeske et al. 2020	pAM383
LwCas13a-msfGFP-2A-Blast	Abudayyeh et al., 2017 (Addgene 91924)	LwaCas13a plasmid
pUC19-U6-LwaCas13acrRNA-BsmBIcassette	This paper	LTH151
human codon optimized Acr construct for AcrVIA4	This paper	LTH956
human codon optimized Acr construct for AcrVIA5	This paper	LTH957
pCMV-T7-AcrIIA4-NLS	Mahendra et at., 2020 (Addgene 133801)	AcrIIA4 construct
pCMV-T7-AcrIIA5-NLS	Mahendra et at., 2020 (Addgene 133802)	AcrIIA5 construct
pCMV-T7-null	Mahendra et at., 2020 (Addgene 171128)	pCMV-null
pUC19-U6-terminator	Addgene 133961	pUC19